Optics Communications 283 (2010) 608–612

Contents lists available at ScienceDirect

Optics Communications

journal homepage: www.elsevier.com/locate/optcom

# Transmitted interference effect of double metallic nanoslits composed of a slit and a square-funnel slit

Ting-Ting Bian [a], Ben-Yuan Gu [b,*], Yan Zhang [c]

[a] Department of Physics, Harbin Institute of Technology, Harbin 150001, PR China
[b] Institute of Physics, Chinese Academy of Sciences, P.O. Box 603, Beijing 100190, PR China
[c] Department of Physics, Capital Normal University, Beijing 100037, PR China

ARTICLE INFO

*Article history:*
Received 3 September 2009
Received in revised form 23 October 2009
Accepted 23 October 2009

*PACS:*
73.20.Mf
42.25.Hz
78.66.−w

*Keywords:*
Surface plasmons
Interference effect
Metallic nanoslits

ABSTRACT

The transmitted interference characteristics for double metallic nanoslits, which are composed of a slit and a square funnel, are investigated by the finite-difference time-domain method. Two types of interference patterns, i.e., the periodic single peak or the periodic double peaks profile, are observed by varying the geometric parameters of the square-funnel slit. The fringe period crucially depends on the exit layer thickness of the square-funnel slit. The near-field field intensity can be enhanced three times that in symmetric slit-doublet structure by selecting specific parameters. We also find that surface plasmon waves can creep along the interface between metal and dielectric, even though the interface possesses orthogonal corners.



## 1. Introduction

Since Ebbesen et al. first discovered the phenomenon of extraordinary optical transmission (EOT) through a two-dimensional hole array perforated on a metallic film in 1998 [1], there has been tremendous interest in the studies of subwavelength metallic structures. More metallic structures, such as single nano-aperture, isolated or dressed with shallow corrugations [2–10], are currently investigated [2–10] to develop diverse applications as well as to understand the underlying physical origins on the EOT. Several mechanisms have been proposed as the possible origins [11–25]. The popular well accepted physical picture is that the EOT effect stems from the excitation of surface plasmon polaritons (SPPs) [18–20] and the Fabry–Perot-type waveguide resonance in apertures [13,15,16]. Further, the fundamentals of the electromagnetic interaction between elementary optical objects, particularly, in slit-doublet experiment at metallic-dielectric interface, also become a significant subject [2–6,26–28]. The in-depth studies of the light interference effects in two slits or a slit and an indention structures have revealed that for a large slit–slit or slit-indention separation, the observation of an oscillatory transmission as a function of the wavelength of the incident light had unambiguously confirmed the SPP-mediated interaction [2], but for much smaller separation distance, the oscillatory feature has dramatically exhibited different behavior [4,8–10] from that driven by the pure SPP mode excitation. It is recently found that the total nearby field scattered on the interface by the nanostructures is not a pure SPP mode, it additionally incorporates a quasi-cylindrical wave (CW), i.e., an electromagnetic field with radiative and evanescent components [27,29]. The CW creeps along the interface over several wavelength distances with an amplitude damping that scales approximately as $1/\sqrt{x}$, where $x$ is the distance away from an abrupt surface discontinuity such as a hole, a bump, a slit edge, etc. It can further interact with other CW generated from nearby nano-aperture as well as the pure SPP waves. Finally, SPP mode, CW and the direct transmitted light (DTL) simultaneously interfere with each other and produce diverse oscillatory modulation patterns in the transmission spectrum and interference fringes.

Currently, Gao et al. provided obvious evidence for SPP-mediated enhanced light transmission through metallic hole arrays [3]. They also showed the dependence of the interference fringes on the film thickness in the slit-doublet structures drilled on a metallic film. There exist two interference fringe periods $\lambda_f$ in the near-field optical images on the output-side surface of the

* Corresponding author. Tel.: +86 10 82649080; fax: +86 10 82649531.
*E-mail addresses:* 13681522860@139.com, ting8386@126.com (T.-T. Bian), guby@aphy.iphy.ac.cn (B.-Y. Gu).

0030-4018/$ - see front matter © 2009 Elsevier B.V. All rights reserved.
doi:10.1016/j.optcom.2009.10.096

structure: $\lambda_f = \lambda_{SPP}/2$ for the thicker film and $\lambda_f = \lambda_{SPP}$ for the thinner film. They proposed that there were two mechanisms involved: one is the interference between SPPs launched by the holes and light transmitted directly through them, creating fringes surrounding individual isolated holes; the other one is the interference between SPPs launched from neighboring holes, forming the interference fringes for hole arrays.

Recently, Shi et al. studied Young's interference of double metallic nanoslits with different widths [6]. They reported that the interference order could be shifted by adjusting the width difference between two slits and indicated this phenomenon could be attributed to the additive phase retardation by the slits. As an application example, Sun and Kim designed metallic lenses consisting of a nanoslit array formed on a metal layer with tapered film thickness [30]. Each nanoslit element of these metallic lenses transmits light with individual phase retardation controlled by variant metal thickness. So the beam focusing and collimating can be realized when appropriately constructing the metallic lenses.

Motivated by these works, in this paper, we present a new structure perforated on a metallic film: a slit and a square funnel. The field distributions on the output-side surface are calculated by the finite-different time-domain (FDTD) method. The metal is treated by the Drude model and the precision of computation has been checked. Two types of interference patterns are observed, i.e., the periodic single peak and the periodic double peaks profile. The near-field magnetic field intensity in specific cases can be three times as that in the symmetric slit-doublet experiment. We also try to clear out the underlying physical mechanism of these novel phenomena. By fitting procedure and analysis, more properties of the SPPs can be found.

## 2. Presentation of the theory

The schematic of calculated structure milled into a gold thin film with a permittivity $\epsilon_m$ is illustrated in Fig. 1. The structure is composed of a simple slit (at the left) and a square-funnel slit (at the right). The overall thickness is denoted by $h$ ($z$-direction) and the width of the left slit is denoted by $w_1$ ($x$-direction). The square-funnel slit consists of an exit slit with a width $w_2$ and a thickness $h_1$ and an entrance with a square section of $w_3(width) \times (h - h_1)(depth)$. The distance between the center of the left slit and the center of the square-funnel slit is $d$. The structure is free-standing in air ($\epsilon_0 = 1.0$) and laid on the $xz$ plane which

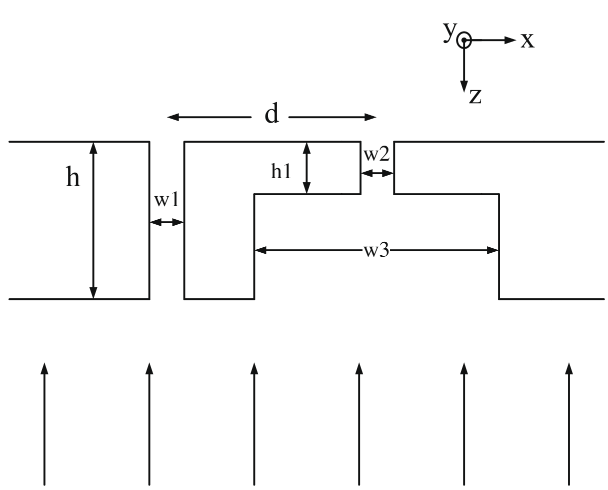


**Fig. 1.** Sketch map of double metallic nanoslits composed of a slit and a square-funnel slit.

is our simulation domain. A vertical plane located on the midline between the two slits corresponds to $x = 0$ and the output surface in our simulation domain corresponds to the $z = 0$ plane. A plane wave light of wavelength $\lambda_0 = 0.633$ μm in vacuum and with the TM-polarization (with the magnetic field parallel to the $y$-axis) impinges normally the structure along the $-z$-direction.

We suppose that the interference at the output interface are due to the comprehensive interactions of DTL, SPPs, and CW. Thus the magnetic field between the two slits on the transmitted surface can be expressed as

$$H_y(x) = A_t e^{i\phi_t}\Theta((x-d_0)/(w_3/2)) + A_{SP1}e^{i\phi_{sp1}}e^{ik_{SP}(x+d_0)} + A_{SP2}e^{i\phi_{sp2}}e^{-ik_{SP}(x-d_0)} + \frac{A_{C1}e^{i\phi_{c1}}}{\sqrt{d_0+x}}e^{ik_0(x+d_0)} + \frac{A_{C2}e^{i\phi_{c2}}}{\sqrt{d_0-x}}e^{-ik_0(x-d_0)} \quad (1)$$

where $d_0 = d/2$ and $\Theta$ represents a window step function, i.e., $\Theta(x/\triangle x) = 1$ for $|x| < \triangle x$ and 0 for others. $A_t$ denotes the amplitude of the DTL. $A_{SP1}$ and $A_{C1}$ represent the amplitudes of SPPs and CW of the left slit while $A_{SP2}$ and $A_{C2}$ emerge from the square-funnel slit at right. The initial phases of $A_t$, $A_{SP1}$, $A_{SP2}$, $A_{C1}$ and $A_{C2}$ are denoted by $\phi_t$, $\phi_{sp1}$, $\phi_{sp2}$, $\phi_{c1}$ and $\phi_{c2}$, respectively. We reckon that the individual phase is originated from our designed asymmetry structure and the fixed phase shift between DTL, SPP and CW. The incident light propagates in air with a wave vector $k_0$ and SPPs travels along the ±$x$-axis with a complex wave vector $k_{SP}$. When the thickness of a metal film is small, we reckon that a part of the incident light can directly transmit through the film, formed DTL. In our model structure it is assumed that the DTL is confined only to a region around the right slit with a width $w_3$, which corresponds to a thin metal layer or air slit. Then the magnetic field intensity distribution between the two slits on the transmitted surface can be derived from Eq. (1) as follows:

$$\begin{aligned} I_{tot}(x) = |H_y(x)|^2 = {} & A_t^2\Theta((x-d_0)/(w_3/2)) + A_{SP1}^2 + A_{SP2}^2 \\ & + \frac{A_{C1}^2}{d_0+x} + \frac{A_{C2}^2}{d_0-x} + 2A_t\Theta((x-d_0)/(w_3/2))A_{SP1}\cos[k_{SP}(x+d_0) \\ & - (\phi_t - \phi_{sp1})] + 2A_t\Theta((x-d_0)/(w_3/2))A_{SP2}\cos[k_{SP}(x-d_0) \\ & + (\phi_t - \phi_{sp2})] + 2A_t\Theta((x-d_0)/(w_3/2))\frac{A_{C1}}{\sqrt{d_0+x}}\cos[k_0(x+d_0) \\ & - (\phi_t - \phi_{c1})] + 2A_t\Theta((x-d_0)/(w_3/2))\frac{A_{C2}}{\sqrt{d_0-x}}\cos[k_0(x-d_0) \\ & + (\phi_t - \phi_{c2})] + 2A_{SP1}\frac{A_{C1}}{\sqrt{d_0+x}}\cos[(k_{sp}-k_0)x + k_{sp}d_0 - k_0d_0 \\ & + (\phi_{sp1} - \phi_{c1})] + 2A_{SP2}\frac{A_{C2}}{\sqrt{d_0-x}}\cos[(k_{sp}-k_0)x - k_{sp}d_0 \\ & + k_0d_0 - (\phi_{sp2} - \phi_{c2})] + 2A_{SP1}\frac{A_{C2}}{\sqrt{d_0-x}}\cos[(k_{sp}+k_0)x \\ & + k_{sp}d_0 - k_0d_0 + (\phi_{sp1} - \phi_{c2})] + 2A_{SP2}\frac{A_{C1}}{\sqrt{d_0+x}}\cos[(k_{sp}+k_0)x \\ & - k_{sp}d_0 + k_0d_0 - (\phi_{sp2} - \phi_{c1})] + 2A_{SP1}A_{SP2}\cos(2k_{sp}x + \phi_{sp1} \\ & - \phi_{sp2}) + 2\frac{A_{C1}}{\sqrt{d_0+x}}\frac{A_{C2}}{\sqrt{d_0-x}}\cos(2k_0x + \phi_{c1} - \phi_{c2}) \end{aligned} \quad (2)$$

Therefore, the magnetic field intensity exhibits cosine oscillations on the output-side surface. Various oscillatory fringe periods can be observed, such as $\lambda_f = \lambda_{SPP}/2$, $\lambda_f = \lambda_{SPP}$, $\lambda_f = \lambda_0/2$, $\lambda_f = \lambda_0$, etc. The phase values of $A_t$, $A_{SP1}$, $A_{SP2}$, $A_{C1}$ and $A_{C2}$ have no impact on the interference fringe period. The relative weight of the amplitudes of the DTL, SPPs and CW dominates the ultimate interference fringe period. Based on the FDTD simulated results, all of the parameters in Eq. (2) can be obtained by the fitting procedures.